9-1-2020

Detecting Mercury (II) and Thiocyanate Using "Turn-on" Fluorescence of Graphene Quantum Dots

Faezeh Askari
University of Zabol

Abbas Rahdar
University of Zabol

Mohadeseh Dashti
University of Windsor

John F. Trant
University of Windsor

Detecting mercury (II) and thiocyanate using "turn-on" fluorescence of graphene quantum dots

Faezeh Askari[a], Abbas Rahdar [a]*, Mohadeseh Dashti [b], John F. Trant [b]*

[a] Department of Physics, University of Zabol, Zabol, P. O. Box. 98613-35856, Iran

[b] Department of Chemistry and Biochemistry, University of Windsor, Windsor, ON, N9B 3P4, Canada

Corresponding author for editorial office:

John Trant j.trant@uwindsor.ca; 519-253-3000 xt 3528

Abstract

In this work, 1.8 nm graphene quantum dots (GQDs), exhibiting bright blue fluorescence, were prepared using a bottom-up synthesis from citric acid. The fluorescence of the GQDs could be almost completely quenched (about 96%) by adding Hg^{2+}. Quenching was far less efficient with other similar heavy metals, Tl^{+}, Pb^{2+} and Bi^{3+}. Fluorescence could be near quantitatively restored through the introduction of thiocyanate. This "turn-on" fluorescence can thus be used to detect both or either environmental and physiological contaminants mercury and thiocyanate and could prove useful for the development of simple point-of-care diagnostics in the future.

Keywords: Graphene quantum dot, Hg^{2+}, SCN^{-}, fluorescent detection.

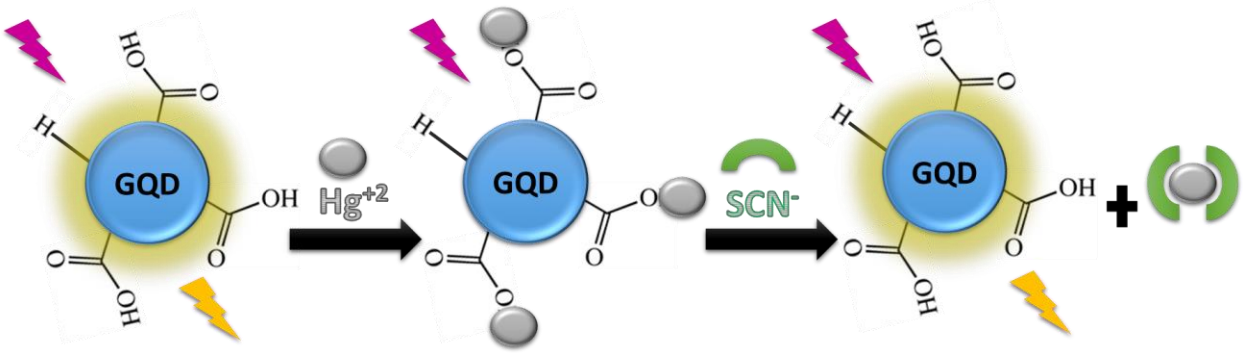

1. Introduction

Environmental and physiological detection of Mercury remains an important health challenge.[1] As it is poorly cleared by the body, it can accumulate in the brain causing neurodegeneration and other chronic conditions through a combination of DNA damage, mitosis impairment and permanent damage to central nervous system signaling. Unfortunately, it is a necessary resource in our industrial economy with total anthropogenic mercury release into the environment estimated at 3000 tons/annum.[2] Physiological and environmental Hg^{2+} level are generally quantified through surface-enhanced Raman scattering,[3] X-ray absorption spectroscopy,[4] atomic absorption spectroscopy,[5] inductively coupled plasma mass spectrometry,[6,7] bacterial-based biosensors,[8] HPLC-cold vapour-atomic fluorescence spectroscopy,[9,10] and, more recently, solution fluorescence detection.[11,12] This last application has significant advantages, including less expensive equipment and faster data acquisition.[13,14] Various small organic[15,16], and inorganic materials[17] have been used to determine Hg^{2+} levels using fluorescence, but fluorescent graphene quantum dots (GQDs) are a promising alternative.[18]

GQDs, defined as near-0-dimensional carbon materials comprising graphene sheets under 100 nm but often below 5 nm, have excellent optical properties and high stability. Unlike their heavy-metal alternatives, their low toxicity and biocompatibility[19] make them interesting tools for use in the environment or for physiological applications.[20] GQD synthesis falls into two main categories: top-down, and bottom-up methods.[21-25] Top-down approaches involve the cutting of larger graphene sheets into GQDs. These are generally robust methods but give less control over the size and dispersity of the resulting dots. This is incredibly important when specific optical properties are sought as the emission λ_{max} is a function of size. In contrast, bottom-up approaches involve the *de novo* synthesis of graphene from non-graphene molecular precursors.[25-27] This strategy allows for the preparation of particles with a well-defined size and low dispersity and is becoming increasingly prevalent and simple. This uniformity makes GQDs promising tools for a wide variety of applications,[28,29] including: as photodetectors for electronics,[30] as photoluminescent probes,[31,32] as biosensors,[33,34] and as biomedical tools for drug delivery, cancer photodiagnostics, and antimicrobial treatment.[35,36] GQD photoactivity sensing largely relies on energy and/or charge transfer from the GQD to adsorbed ligands to quench the innate fluorescence of the GQDs. A good example is the work of Sun's group at Changchun, who used GQDs derived from grass for the detection of Cu^{2+} by quenching the innate fluorescence of the dots.[37] However,

this “turn-off” principle usually suffers from relatively low sensitivity (as was the case with Sun’s work where Cu only quenched 25% of the fluorescence),[37] and is susceptible to complications from impurities or other analytes (in this same example, iron quenched 10%, mercury 5%, and other metals lower levels), leading to false positives. This turn-off approach has likewise been employed for mercury with similar challenges, albeit with generally better selectivity for mercury over other metals.[12,38-41] In contrast, “turn on” fluorescence sensors, which involve one ligand inactivating the GQD, and a second restoring the fluorescence, are more reliable due to the “two factor authentication” mechanism, and have now been extensively developed.[42-46] For example, Tian’s group has used this approach to detect copper ions (Cu^{2+}) with good selectivity and sensitivity.[46] Qu and co-workers at Changchun used this approach to detect bithiols and Hg^{2+} in water,[47] and Ye and colleagues at Nanjing used a nitrogen-doped quantum dot to improve sensitivity for the same application.[48] Huang and colleagues used a similar technique, employing either iodide or L-cysteine to restore the fluorescence of nitrogen-doped carbon quantum dots and to act as a concentration-sensitive sensor of either mercury or iodide/cysteine,[11] and Kokot and coworkers used the same strategy to show that it works with undoped GQDs.[49] and Wu and Tong employed ammonium citrate/cysteine-derived sulfur-nitrogen co-doped nanoparticles to detect both mercury and sulfides.[50]

Elevated levels of thiocyanate (SCN^-) can lead to endemic goiter, tropical diabetes, ataxic neuropathy, infantile myxedema. This is generally related to dietary consumption of cyanogenic glycosides contained in food, particularly some vegetables.[51] Higher SCN- levels in urine also act as a biomarker of increased metabolism and cancer,[52] and is the common biomarker for identifying possible cyanide poisoning where analysis needs to be done very quickly.[53] Although exposure may have increased in an industrial society, SCN- has always been in the diet, and it is the substrate for the human defensive peroxidases.[54]

For these reasons, determining the level of SCN^- in a sample has multiple medical applications, driving the development of fluorescent sensors. Das and co-workers identified a rhodamine derivative that forms a salt selectively with thiocyanate to turn-on fluorescence;[55] similarly, Yang, Lin and coworkers showed that a fluorene-derived dimeric structure could have fluorescent intramolecular charge transfer interrupted by the presence (and nucleophilic attack) of thiocyanate to turn off the effect.[56] The Chen lab in Shandong noted that gold nanoparticles could be induced to aggregate by the addition of SCN^- changing the colour of the solution from red to

blue, and only cyanide showed interference;[57] while Dai and coworkers at Nanjing made gold nanostars that change colour in the presence of thiocyanate.[58] Yang at Changchun showed that with a cystamine-functionalized nanoparticle, the colour change could even indicate SCN concentration.[59] Ma and Wu at Nanchang developed an ultrasensitive (0.09 nM) tool for detecting isothiocyanate relying on FRET between fluorescein and gold nanoparticles.[60] Yang and Yang at Changchun adsorbed graphene quantum dots onto gold nanoparticles that quenched the fluorescence of the nanoparticles by inducing aggregation.[61] Thiocyanate interrupts this process by outcompeting the GQDs and leaving the fluorescence turned "on." Many of these strategies rely on the interaction between thiocyanate and gold. GQDs are potentially less expensive, and thiocyanate also shows high affinity for mercury ions which in turn show high affinity for carboxylated-graphene quantum dots through salt formation. Mercury also shows higher affinity for carboxylates than other heavy metals, meaning that the system should be selective.[62] This is a promising chain of interactions. However, there are no examples of GQDs being screened for fluorescence recovery, dual Hg^{+}/SCN^{-} detection. The promise of this potential inspired us to explore it in this study.

2. Experimental

2.1. Materials

Citric acid, sodium hydroxide, sodium thiocyanate, thallium(I) nitrate, mercury(II) nitrate, lead(II) nitrate, and bismuth(III) nitrate were purchased from Merck KGaA. Double distilled water was used throughout the experiment.

2.2. Equipment

Fourier transform infrared (FT-IR) spectra were obtained on a Perkin-Elmer Spectrum RXI FT-IR spectrophotometer. Ultraviolet-visible light (UV-Vis) absorption spectra were recorded by a Perkin Elmer UV/Vis spectrophotometer. All fluorescent spectra were obtained with an FL spectrophotometer (Shimadzu RF-6000). The AFM image was obtained in non-contact mode (Ara Research, Iran). To prepare the sample, an aqueous solution of GQDs (10 μL) was dropped onto the surface of a freshly exfoliated mica substrate. After drying, the AFM image was recorded. The FE-SEM image of the same prepared sample was obtained by field emission scanning electron

microscope (FE-SEM; Mira 3-XMU). All optical measurements were carried out in quartz cuvettes at ambient temperature.

2.3. Synthesis of graphene quantum dots (GQDs)

The GQDs were made by pyrolyzing the carbon precursors using the approach of Li and coworkers,[63] incorporating our previously published modifications:[64] one gram of citric acid was put into a beaker and heated to 200 °C on a hot plate (Corning). The citric acid fully melted after 5 min and the liquid turned yellow. After an additional 10 minutes of heating, the liquid became orange, indicating the formation of GQDs, and the beaker was removed from the heat and cooled to ambient. Consequently, a total reaction time of 14 min was used; additional heating can lead to the formation of graphene oxides which are difficult to separate from the GQDs. The reaction mixture was adjusted to pH 7 with NaOH (12 ml, 1M) to provide a solution of the GQDs in water (approximately 12 mL). These were dialyzed (3500 MWCO) against distilled water (20 mL). The dialysate in the beaker turned orange and was collected and stored. The tube was then redistilled against a fresh 20 mL of water. The dialysis tube and its contents were then discarded. The combined dialysates were then dialyzed against water (100 mL, 1000 MWCO) with two changes of water to remove any residual citric acid or small oligomers. The contents of the tube (approx. 40 mL) were then lyophilized to provide GQDs as a powder that could be stored at -20 ºC until needed.

2.4. Fluorescence quenching by heavy metal nitrates

GQDs were resuspended in PBS (1 mg·ml^{-1} in 1x PBS) and a 3 mL aliquot was transferred to a quartz cuvette to which was added 10 µL of aqueous Mercury(II) nitrate (1 M) was added and the fluorescence spectra were recorded at ambient temperature at an excitation wavelength of 360 nm. To confirm the selectivity of Hg^{2+}-mediated quenching of GQDs, the process was repeated for each of thallium(I), Lead(II), and Bismuth(III) nitrates (all at 1 M, 10 µL). Final concentrations of analytes is 3.3 µM with 1 mg/mL of GQDs. The initial spectrum was recorded as was the associated fluorescently quenched spectrum for each sample.

2.5. Using “turn-on” fluorescence for the detection of SCN^- using Hg^{2+}@GQDs

The fluorescence of the samples, at 360 nm excitation, was measured for a 3 ml aliquot of the GQD solution (1 mg/mL in PBS) mixed with 10 µL of the aqueous mercury (II) nitrate (1 M).

Then 10 µL of sodium thiocyanate (1 M) was added to the cuvette and mixed with pipetting. Final concentrations of analytes is 3.3 µM with 1 mg/mL of GQD. The emission spectrum of this solution was then also recorded with an excitation wavelength of 360 nm.

3. Results and Discussion

3.1. FTIR analysis

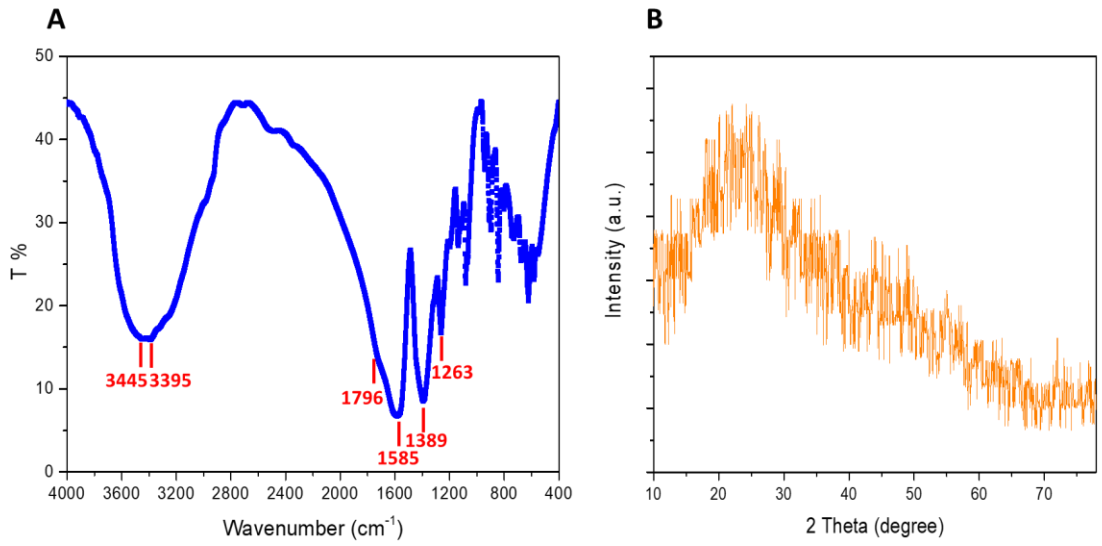

Figure 1. **A)** FT-IR spectrum and **B)** XRD of the GQDs.

FT-IR analysis confirms the presence of the expected carboxylate functionalities in the GQDs, showing the characteristic stretching vibrations of carboxyl and hydroxyl groups at 3600-3300 cm^{-1} and the asymmetric and symmetric carboxyl stretches at 1585 and 1389 cm^{-1} respectively (Figure 1A). These acids will be involved in binding the mercury ions. We also see the expected aliphatic C=C stretches at lower wavenumbers indicative of the presence of aromatics in the graphene. The powder X-ray analysis is also typical of graphene with a low intensity and broad 2θ value of approximately 23 degrees for the 002 face (Figure 1B).[65]

3.2. FSEM analysis

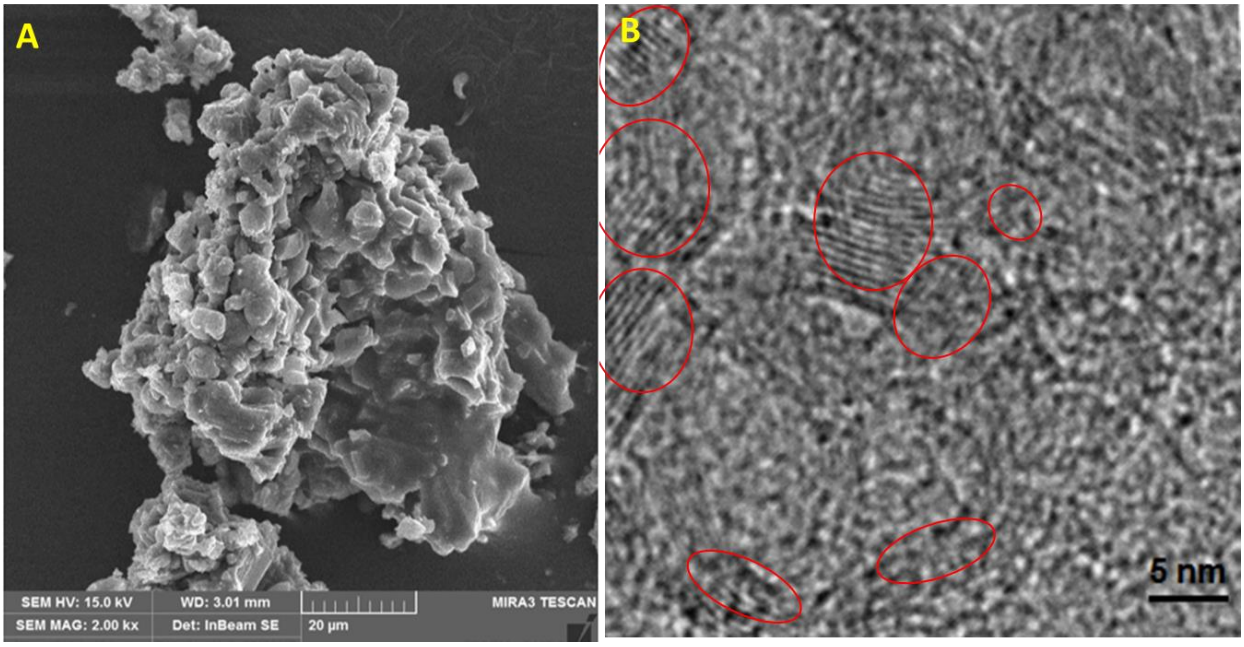

Figure 2. A) FESEM and **B)** HRTEM images of the GQDs on mica

The FESEM images provide images of the dried aggregates formed by the GQDs, but as the resolution of the instrument (20 µm) is orders of magnitude greater than the size of the particles (about 2 nm) but it still shows evidence that we are seeing aggregation rather than the presence of bulk materials (Figure 2A). This was also proven by synthesis, as the only particles retained are those that can pass through 3500 MWCO dialysis tubing but be retained by 1000 MWCO membranes. The HRTEM on the other hand shows clear evidence of the nanoparticles at the expected sizes and are represented as areas containing parallel lines as has been noted previously in the literature (Figure 2B).[64,66-70]

3.4. AFM analysis

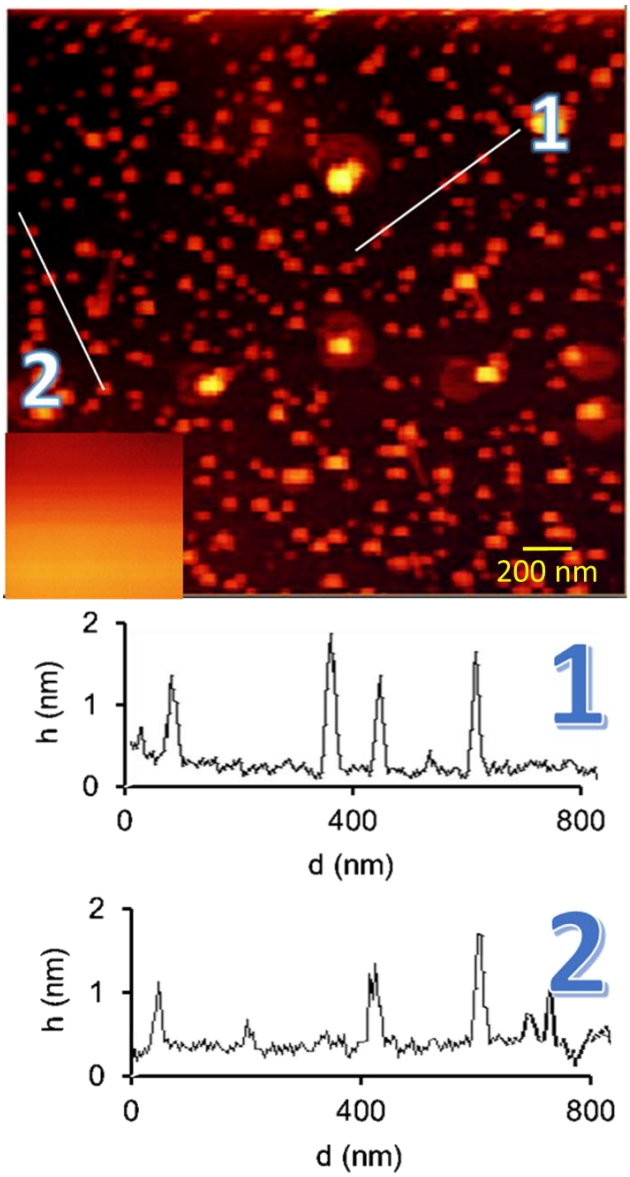

Figure 3. AFM-acquired image of the GQDs and the height graph of a representative cross-section of the image, corner of the picture shows the AFM image of the unfunctionalized mica surface.

GQDs were then characterized using atomic force microscopy (AFM, Figure 3). The average size of the GQDs was calculated to be 1.8 nm based on the height of 50 particles from different images. This sizing is consistent with experimental expectations, the synthetic and purification conditions, and the HRTEM image. It is also largely consistent with the expected emission for particles of this size considering the differential functionalization.[71] The AFM image suggests that the dispersity of the samples is low: the larger objects are likely the result of aggregation occurring on the surface of the mica substrate.

3.5. Spectrometric analysis

The GQDs show a well-defined absorption band at 360 nm (Figure 4A); their maximum excitation and emission wavelengths are at 360 and 460 nm, respectively. The fluorescence intensity however is highly dependent on the presence of cations in solution (Figure 4B). All examined heavy metals, Tl^{+}, Pb^{2+}, Bi^{3+} and Hg^{2+}, at least partially quenched GQD fluorescence emission: by about 10%, 52%, 70%, and 96% respectively. With the potential exception of bismuth,[72] all of these metals are toxic as they disrupt enzymatic function;[73] however, the reduction of environmental lead,[74,75] and the thankfully low levels of environmental thallium,[76] mean that detection of mercury is likely the most relevant application, aided by the high sensitivity of system for this metal over the others.

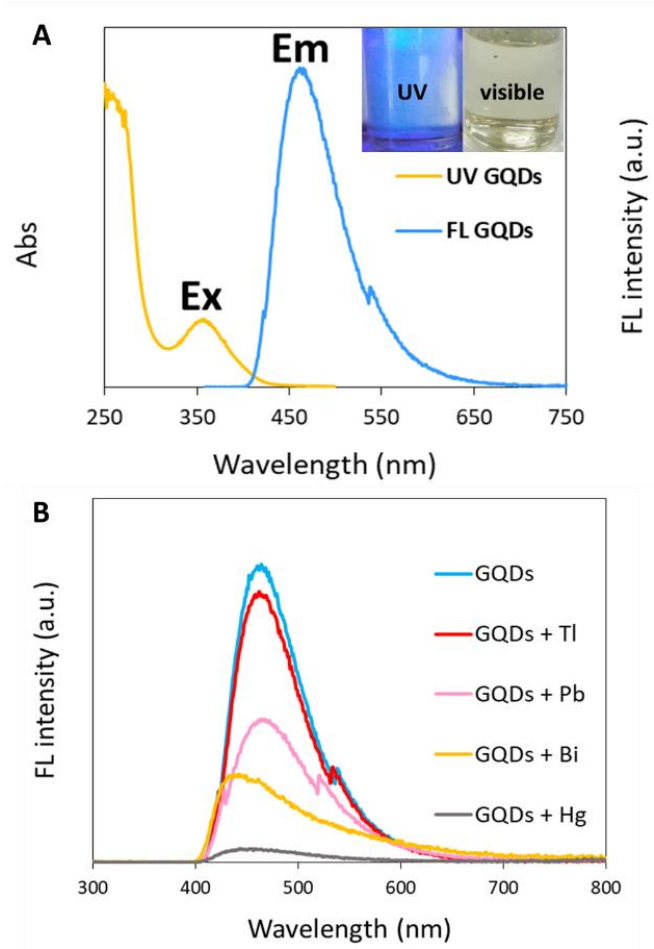

Figure 4. **A)** UV-Vis and fluorescent spectra, fluorescence excitation (λ_{em} = 461 nm) and emission (λ_{ex} = 360 nm), of the GQDs. Inset: Photographs acquired both under UV-lamp irradiation and

under normal lighting conditions. **B)** Emission spectra of GQDs alone (blue) and in the presence of equal concentrations (3.3 μM) of Tl^{+} (red), Pb^{2+} (pink), Bi^{3+} (yellow) and Hg^{2+} (grey).

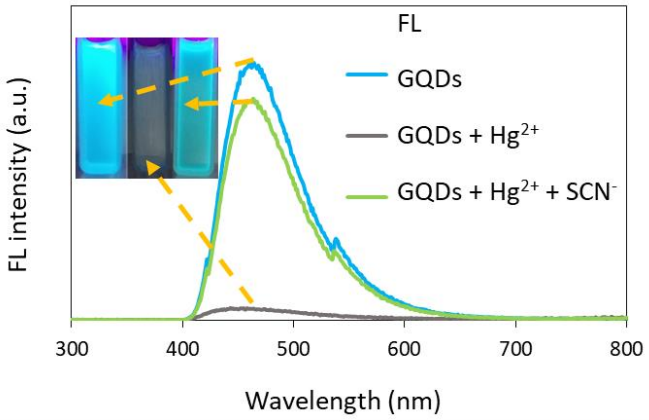

Figure 5. Fluorescence emission spectrum of the GQD solution (blue); GQDs in the presence of 3.3 μM Hg^{+2} (grey); and GQDs in the presence of 3.3 μM Hg^{+2} followed by 3.3 μM SCN^{-} (green). Inset: Photographs of each solution under UV illumination.

The very high quenching efficiency of Hg^{2+} is likely due to the very high affinity of mercury for carboxylates. The selectivity of mercury over other heavy metals for carboxylates is well established.[77-79] However, at the concentrations used, the GQDs are likely saturated in all cases: the fluorescence quenching is due to the specific nature of the mercury ion, and is effectively quantitative in the presence of Hg^{2+}. However, Hg^{2+} is known to bind far more strongly to SCN^{-} than to a carboxylate.[80] Consequently, in the presence of the thiocyanate, the Hg^{2+} ions desorb from the GQD surface, almost completely restoring the fluorescence of the particles (Figure 5). This reversibility is potentially useful.

Conclusion:

Carboxylate-functionalized GQDs with a diameter of 1.8 nm were synthesized using a bottom-up strategy from citric acid and characterized by AFM, FT-IR and TEM. When exposed to heavy metals, the fluorescence was quenched only in the presence of Hg^{2+} making them a potentially useful sensor. Fluorescence is readily restored by the addition of thiocyanate. The very simple synthesis of these materials coupled with the “turn-on” detector for both mercury and thiocyanate, pollutants of concern, shows the versatility of this approach and these materials.

Acknowledgements: A. Rahdar would like to thank the University of Zabol for financial support (UOZ-GR-9618-40) for this work. J.F. Trant would like to thank the Natural Sciences and Engineering Research Council of Canada (2018-06338) and the Tricouncil's New Frontiers Exploration Grant (NFRFE-2018-00075) for providing financial support for this work. The authors declare no conflicts of interest.

References

1 Clarkson, T. W. & Magos, L. The toxicology of mercury and its chemical compounds. *Crit. Rev. Toxicol.* **36**, 609-662, (2006).

2 Yan, F. *et al.* Highly photoluminescent carbon dots-based fluorescent chemosensors for sensitive and selective detection of mercury ions and application of imaging in living cells. *Sens. Actuators, B* **192**, 488-495, (2014).

3 Guerrini, L. *et al.* Chemical speciation of heavy metals by surface-enhanced Raman scattering spectroscopy: identification and quantification of inorganic- and methyl-mercury in water. *Nanoscale* **6**, 8368-8375, (2014).

4 Kim, C. S., Brown, G. E. & Rytuba, J. J. Characterization and speciation of mercury-bearing mine wastes using X-ray absorption spectroscopy. *Sci. Total Environ.* **261**, 157-168, (2000).

5 Hatch, W. R. & Ott, W. L. Determination of submicrogram quantities of mercury by atomic absorption spectrophotometry. *Anal. Chem.* **40**, 2085-2087, (1968).

6 Lewen, N., Mathew, S., Schenkenberger, M. & Raglione, T. A rapid ICP-MS screen for heavy metals in pharmaceutical compounds. *J. Pharm. Biomed. Anal.* **35**, 739-752, (2004).

7 Wang, M. *et al.* Development of a mild mercaptoethanol extraction method for determination of mercury species in biological samples by HPLC–ICP-MS. *Talanta* **71**, 2034-2039, (2007).

8 Hansen, L. H. & Sørensen, S. J. Versatile biosensor vectors for detection and quantification of mercury. *FEMS Microbiol. Lett.* **193**, 123-127, (2000).

9 Ramalhosa, E., Río Segade, S., Pereira, E., Vale, C. & Duarte, A. Simple methodology for methylmercury and inorganic mercury determinations by high-performance liquid chromatography–cold vapour atomic fluorescence spectrometry. *Anal. Chim. Acta* **448**, 135-143, (2001).

10 Vieira, M. A., Ribeiro, A. S., Curtius, A. J. & Sturgeon, R. E. Determination of total mercury and methylmercury in biological samples by photochemical vapor generation. *Anal. Bioanal. Chem.* **388**, 837-847, (2007).

11 Huang, H. *et al.* Nitrogen-doped carbon quantum dots as fluorescent probe for "off-on" detection of mercury ions, l-cysteine and iodide ions. *J. Colloid Interface Sci.* **506**, 373-378, (2017).

12 Wang, B., Zhuo, S., Chen, L. & Zhang, Y. Fluorescent graphene quantum dot nanoprobes for the sensitive and selective detection of mercury ions. *Spectrochim. Acta, Part A* **131**, 384-387, (2014).

13 Ding, X. *et al.* Highly sensitive SERS detection of Hg^{2+} ions in aqueous media using gold nanoparticles/graphene heterojunctions. *ACS Appl. Mater. Interfaces* **5**, 7072-7078, (2013).

14 Nolan, E. M. & Lippard, S. J. Tools and tactics for the optical detection of mercuric ion. *Chem. Rev.* **108**, 3443-3480, (2008).

15 Kim, I.-B. & Bunz, U. H. F. Modulating the sensory response of a conjugated polymer by proteins: An agglutination assay for mercury ions in water. *J. Am. Chem. Soc.* **128**, 2818-2819, (2006).

16 Gu, Z., Zhao, M., Sheng, Y., Bentolila, L. A. & Tang, Y. Detection of mercury ion by infrared fluorescent protein and its hydrogel-based paper assay. *Anal. Chem.* **83**, 2324-2329, (2011).
17 Shibu, E. S., Hamada, M., Murase, N. & Biju, V. Nanomaterials formulations for photothermal and photodynamic therapy of cancer. *J. Photochem. Photobiol., C* **15**, 53-72, (2013).
18 Sun, X. & Lei, Y. Fluorescent carbon dots and their sensing applications. *TrAC, Trends Anal. Chem.* **89**, 163-180, (2017).
19 Nikazar, S. *et al.* Revisiting the cytotoxicity of quantum dots: An in-depth overview. *Biophys. Rev.*, (2020).
20 Baker, S. N. & Baker, G. A. Luminescent carbon nanodots: Emergent nanolights. *Angew. Chem. Int. Ed.* **49**, 6726-6744, (2010).
21 Li, Y. *et al.* An electrochemical avenue to green-luminescent graphene quantum dots as potential electron-acceptors for photovoltaics. *Adv. Mater. (Weinheim, Ger.)* **23**, 776-780, (2011).
22 Pan, D., Zhang, J., Li, Z. & Wu, M. Hydrothermal route for cutting graphene sheets into blue-luminescent graphene quantum dots. *Adv. Mater. (Weinheim, Ger.)* **22**, 734-738, (2010).
23 Peng, J. *et al.* Graphene quantum dots derived from carbon fibers. *Nano letters* **12**, 844-849, (2012).
24 Essig, S. *et al.* Phonon-assisted electroluminescence from metallic carbon nanotubes and graphene. *Nano Lett.* **10**, 1589-1594, (2010).
25 Liu, R., Wu, D., Feng, X. & Müllen, K. Bottom-up fabrication of photoluminescent graphene quantum dots with uniform morphology. *J. Am. Chem. Soc.* **133**, 15221-15223, (2011).
26 Cai, J. *et al.* Atomically precise bottom-up fabrication of graphene nanoribbons. *Nature* **466**, 470-473, (2010).
27 Lin, L. *et al.* A facile synthesis of highly luminescent nitrogen-doped graphene quantum dots for the detection of 2,4,6-trinitrophenol in aqueous solution. *Nanoscale* **7**, 1872-1878, (2015).
28 Xu, Q. *et al.* Function-driven engineering of 1D carbon nanotubes and 0D carbon dots: mechanism, properties and applications. *Nanoscale* **11**, 1475-1504, (2019).
29 Li, M., Chen, T., Gooding, J. J. & Liu, J. Review of carbon and graphene quantum dots for sensing. *ACS Sensors* **4**, 1732-1748, (2019).
30 Koppens, F. H. L. *et al.* Photodetectors based on graphene, other two-dimensional materials and hybrid systems. *Nat. Nanotechnol.* **9**, 780-793, (2014).
31 Shamsipur, M., Barati, A. & Karami, S. Long-wavelength, multicolor, and white-light emitting carbon-based dots: Achievements made, challenges remaining, and applications. *Carbon* **124**, 429-472, (2017).
32 Zheng, P. & Wu, N. Fluorescence and sensing applications of graphene oxide and graphene quantum dots: A review. *Chem. – Asian J.* **12**, 2343-2353, (2017).
33 Farka, Z., Juřík, T., Kovář, D., Trnková, L. & Skládal, P. Nanoparticle-based immunochemical biosensors and assays: Recent advances and challenges. *Chem. Rev.* **117**, 9973-10042, (2017).
34 Krishnan, S. K., Singh, E., Singh, P., Meyyappan, M. & Nalwa, H. S. A review on graphene-based nanocomposites for electrochemical and fluorescent biosensors. *RSC Adv.* **9**, 8778-8881, (2019).
35 Li, K. *et al.* Technical synthesis and biomedical applications of graphene quantum dots. *J. Mater. Chem. B* **5**, 4811-4826, (2017).
36 Iannazzo, D., Ziccarelli, I. & Pistone, A. Graphene quantum dots: Multifunctional nanoplatforms for anticancer therapy. *J. Mater. Chem. B* **5**, 6471-6489, (2017).
37 Liu, S. *et al.* Hydrothermal treatment of grass: a low-cost, green route to nitrogen-doped, carbon-rich, photoluminescent polymer nanodots as an effective fluorescent sensing platform for label-free detection of Cu(II) ions. *Adv. Mater. (Weinheim, Ger.)* **24**, 2037-2041, (2012).
38 Li, L., Yu, B. & You, T. Nitrogen and sulfur co-doped carbon dots for highly selective and sensitive detection of Hg (Ⅱ) ions. *Biosens. Bioelectron.* **74**, 263-269, (2015).

39 Abdolmohammad-Zadeh, H. & Rahimpour, E. A novel chemosensor based on graphitic carbon nitride quantum dots and potassium ferricyanide chemiluminescence system for Hg(II) ion detection. *Sens. Actuators, B* **225**, 258-266, (2016).

40 Anh, N. T. N., Chowdhury, A. D. & Doong, R.-a. Highly sensitive and selective detection of mercury ions using N, S-codoped graphene quantum dots and its paper strip based sensing application in wastewater. *Sens. Actuators, B* **252**, 1169-1178, (2017).

41 Yang, Y. *et al.* The fluorescent quenching mechanism of N and S co-doped graphene quantum dots with Fe^{3+} and Hg^{2+} ions and their application as a novel fluorescent sensor. *Nanomaterials* **9**, 738, (2019).

42 Zhang, L., Peng, D., Liang, R.-P. & Qiu, J.-D. Graphene quantum dots assembled with metalloporphyrins for "Turn On" sensing of hydrogen peroxide and glucose. *Chem. - Eur. J.* **21**, 9343-9348, (2015).

43 Ananthanarayanan, A. *et al.* Facile synthesis of graphene quantum dots from 3D graphene and their application for Fe^{3+} sensing. *Adv. Funct. Mater.* **24**, 3021-3026, (2014).

44 Chen, C., Zhao, D., Hu, T., Sun, J. & Yang, X. Highly fluorescent nitrogen and sulfur co-doped graphene quantum dots for an inner filter effect-based cyanide sensor. *Sens. Actuators, B* **241**, 779-788, (2017).

45 Li, L. *et al.* Graphene quantum dots as fluorescence probes for turn-off sensing of melamine in the presence of Hg^{2+}. *ACS Appl. Mater. Interfaces* **6**, 2858-2864, (2014).

46 Qu, Q., Zhu, A., Shao, X., Shi, G. & Tian, Y. Development of a carbon quantum dots-based fluorescent Cu^{2+} probe suitable for living cell imaging. *Chem. Commun.* **48**, 5473-5475, (2012).

47 Zhou, L., Lin, Y., Huang, Z., Ren, J. & Qu, X. Carbon nanodots as fluorescence probes for rapid, sensitive, and label-free detection of Hg^{2+} and biothiols in complex matrices. *Chem. Commun.* **48**, 1147-1149, (2012).

48 Yan, Z. *et al.* A green synthesis of highly fluorescent nitrogen-doped graphene quantum dots for the highly sensitive and selective detection of mercury (II) ions and biothiols. *Anal. Meth.* **8**, 1565-1571, (2016).

49 Li, Z., Wang, Y., Ni, Y. & Kokot, S. A rapid and label-free dual detection of Hg (II) and cysteine with the use of fluorescence switching of graphene quantum dots. *Sens. Actuators, B* **207**, 490-497, (2015).

50 Wu, H. & Tong, C. Nitrogen- and sulfur-codoped carbon dots for highly selective and sensitive fluorescent detection of Hg^{2+} ions and sulfide in environmental water samples. *J. Agric. Food Chem.* **67**, 2794-2800, (2019).

51 Saussereau, E., Goullé, J.-P. & Lacroix, C. Determination of thiocyanate in plasma by ion chromatography and ultraviolet detection. *J. Anal. Toxicol.* **31**, 383-387, (2007).

52 Shiue, I. Urinary thiocyanate concentrations are associated with adult cancer and lung problems: US NHANES, 2009-2012. *Environ. Sci. Pollut. Res. Int.* **22**, 5952-5960, (2015).

53 Logue, B. A., Hinkens, D. M., Baskin, S. I. & Rockwood, G. A. The analysis of cyanide and its breakdown products in biological samples. *Crit. Rev. Anal. Chem.* **40**, 122-147, (2010).

54 Ashby, M. T. Inorganic chemistry of defensive peroxidases in the human oral cavity. *J. Dent. Res.* **87**, 900-914, (2008).

55 Banerjee, A. *et al.* A rhodamine derivative as a "lock" and SCN^- as a "key": Visible light excitable SCN^- sensing in living cells. *Chem. Commun.* **49**, 2527-2529, (2013).

56 Yang, T. *et al.* Novel fluorene-based fluorescent probe with excellent stability for selective detection of SCN^- and its applications in paper-based sensing and bioimaging. *J. Mater. Chem. B* **7**, 4649-4654, (2019).

57 Zhang, Z. *et al.* Label free colorimetric sensing of thiocyanate based on inducing aggregation of Tween 20-stabilized gold nanoparticles. *Analyst* **137**, 2682-2686, (2012).

58 Cui, X. *et al.* Highly sensitive and selective colorimetric sensor for thiocyanate based on electrochemical oxidation-assisted complexation reaction with gold nanostars etching. *J. Hazard. Mater.* **391**, 122217, (2020).
59 Zhang, J., Yang, C., Wang, X. & Yang, X. Colorimetric recognition and sensing of thiocyanate with a gold nanoparticle probe and its application to the determination of thiocyanate in human urine samples. *Anal. Bioanal. Chem.* **403**, 1971-1981, (2012).
60 Song, J., Wu, F.-Y., Wan, Y.-Q. & Ma, L.-H. Ultrasensitive turn-on fluorescent detection of trace thiocyanate based on fluorescence resonance energy transfer. *Talanta* **132**, 619-624, (2015).
61 Zhao, D., Chen, C., Lu, L., Yang, F. & Yang, X. A dual-mode colorimetric and fluorometric "light on" sensor for thiocyanate based on fluorescent carbon dots and unmodified gold nanoparticles. *Analyst* **140**, 8157-8164, (2015).
62 Deb, C. & Basu, B. Selectivity of mercury(II) salts in reactions with α,β-unsaturated stannyl esters. *J. Organometal. Chem.* **443**, C24-C25, (1993).
63 Wang, S., Chen, Z.-G., Cole, I. & Li, Q. Structural evolution of graphene quantum dots during thermal decomposition of citric acid and the corresponding photoluminescence. *Carbon* **82**, 304-313, (2015).
64 Askari, F., Rahdar, A. & Trant, J. F. l-tryptophan adsorption differentially changes the optical behaviour of pseudo-enantiomeric cysteine-functionalized quantum dots: Towards chiral fluorescent biosensors. *Sens. Bio-sens. Res.* **22**, 100251, (2019).
65 Kumar, S. *et al.* Tunable (violet to green) emission by high-yield graphene quantum dots and exploiting its unique properties towards sun-light-driven photocatalysis and supercapacitor electrode materials. *Mater. Tod. Commun.* **11**, 76-86, (2017).
66 Dong, Y. *et al.* Blue luminescent graphene quantum dots and graphene oxide prepared by tuning the carbonization degree of citric acid. *Carbon* **50**, 4738-4743, (2012).
67 Sahu, S., Behera, B., Maiti, T. K. & Mohapatra, S. Simple one-step synthesis of highly luminescent carbon dots from orange juice: application as excellent bio-imaging agents. *Chem. Commun.* **48**, 8835-8837, (2012).
68 Tang, L. *et al.* Deep ultraviolet photoluminescence of water-soluble self-passivated graphene quantum dots. *ACS Nano* **6**, 5102-5110, (2012).
69 Zhang, H. *et al.* Carbon quantum dots/Ag_3PO_4 complex photocatalysts with enhanced photocatalytic activity and stability under visible light. *J. Mater. Chem.* **22**, 10501-10506, (2012).
70 Ming, H. *et al.* Large scale electrochemical synthesis of high quality carbon nanodots and their photocatalytic property. *Dalton Trans.* **41**, 9526-9531, (2012).
71 Sk, M. A., Ananthanarayanan, A., Huang, L., Lim, K. H. & Chen, P. Revealing the tunable photoluminescence properties of graphene quantum dots. *J. Mater. Chem. C* **2**, 6954-6960, (2014).
72 Mohan, R. Green bismuth. *Nat. Chem.* **2**, 336-336, (2010).
73 Babula, P. *et al.* Uncommon heavy metals, metalloids and their plant toxicity: A review. *Environ. Chem. Lett.* **6**, 189-213, (2008).
74 Tsoi, M.-F., Cheung, C.-L., Cheung, T. T. & Cheung, B. M. Y. Continual decrease in blood lead level in Americans: United States National Health Nutrition and Examination Survey 1999-2014. *Am. J. Med.* **129**, 1213-1218, (2016).
75 Ysart, G. *et al.* 1997 UK Total Diet Study dietary exposures to aluminium, arsenic, cadmium, chromium, copper, lead, mercury, nickel, selenium, tin and zinc. *Food Addit. Contam.* **17**, 775-786, (2000).
76 Belzile, N. & Chen, Y.-W. Thallium in the environment: A critical review focused on natural waters, soils, sediments and airborne particles. *Appl. Geochem.* **84**, 218-243, (2017).

77 Rambaud, L. *et al.* Influence of monosubstitution of hexakis(3,6-anhydro)cyclomaltohexaose on its complexation properties with ions, with special attention to heavy metals. *Eur. J. Org. Chem.* **2006**, 1245-1250, (2006).
78 Salahuddin, A. Interaction of mercury (II) with organic acids a conductometric study. *J. Prakt. Chem. (Weinheim, Ger.)* **37**, 290-297, (1968).
79 Rossotti, F. J. C. & Whewell, R. J. Structure and stability of carboxylate complexes. Part 16. Stability constants of some mercury (II) carboxylates. *J. Chem. Soc., Dalton Trans.*, 1223-1229, (1977).
80 Achadu, O. J. & Nyokong, T. Graphene quantum dots anchored onto mercaptopyridine-substituted zinc phthalocyanine-Au@Ag nanoparticle hybrid: Application as fluorescence "off-on-off" sensor for Hg^{2+} and biothiols. *Dyes Pigm.* **145**, 189-201, (2017).